



## Head Injury Analysis of Vehicle Occupant in Frontal Crash Simulation: Case Study of ITB's Formula SAE Race Car

Sandro Mihradi<sup>1,\*</sup>, Hari Golfianto<sup>1</sup>, Andi Isra Mahyuddin<sup>1</sup> & Tatacipta Dirgantara<sup>2</sup>

<sup>1</sup>Mechanical Design Research Group, Mechanical Engineering Department, Faculty of Mechanical and Aerospace Engineering, Institut Teknologi Bandung, Jalan Ganesha 10, Bandung 41032, Indonesia

<sup>2</sup>Lightweight Structures Research Group, Aeronautics & Astronautics Department Faculty of Mechanical and Aerospace Engineering, Institut Teknologi Bandung Jalan Ganesha 10, Bandung 41032, Indonesia  
E-mail: sandro@ftmd.itb.ac.id

**Abstract.** In the present study, frontal crash simulations were conducted to determine the effect of various car speeds against the Head Injury Criterion (HIC), a measure of the likelihood of head injury arising from impact. The frontal impact safety of ITB's formula SAE race car designed by students was evaluated as a case study. LS-DYNA<sup>®</sup>, an explicit finite element code for non-linear dynamic analysis was utilized in the analysis. To analyze head injury, a two-step simulation was conducted. In the first step, a full-frontal barrier test was simulated without incorporating a dummy inside the car. The output was the deceleration data of the car, which was used as input in the second step, a sled test simulation. In the sled test, only the cockpit and dummy were modeled. The effect of deceleration to the head of the dummy was then evaluated. The results show that HIC values at an impact speed of 7 m/s (25 km/h) to 11 m/s (40 km/h) were below the safe limit and still in the safe zone. However, the HIC values will exceed the safe limit when the speed of impact is the same as or greater than 12 m/s (43 km/h).

**Keywords:** *finite element analysis; frontal collision; FSAE; head injury; impact attenuator; sled test.*

### 1 Introduction

The Society of Automotive Engineers (SAE) hosts a number of student design competitions, one of which is Formula SAE<sup>®</sup>, which challenges students to design a formula-style race car. One of the essential aspects is safety, especially in the impact attenuator (IA) and seatbelt design. The IA absorbs kinetic energy during frontal impact, while the seatbelt restrains the driver's body from moving forward due to deceleration. According to the 2013 Formula SAE Rules [1], the IA has to be able to absorb sufficient impact energy, i.e. when mounted

---

Received May 8<sup>th</sup>, 2017, Revised October 13<sup>th</sup>, 2017, Accepted for publication October 30<sup>th</sup>, 2017.

Copyright ©2017 Published by ITB Journal Publisher, ISSN: 2337-5779, DOI: 10.5614/j.eng.technol.sci.2017.49.4.8

on the front of a vehicle with a total mass of 300 kgs (661 lbs) that runs into a solid, non-yielding impact barrier with an impact velocity of 7.0 meters/second (23.0 ft/sec), it will give an average deceleration of the vehicle not exceeding 20 G, with peak deceleration less than or equal to 40 G. Total energy absorbed must equal or exceed 7350 joules.

Vehicle collision can cause mild to severe injuries and even fatality. Statistically, frontal collisions are the main cause of fatality during motor vehicle accidents [2]. Common injuries that can be caused by frontal collision are head injuries, thoracic injuries, and internal injuries. Studies on accidental injuries have been reported in many works [3-11]. Head injury assessment can be made by measuring the Head Injury Criterion (HIC) value, a measure of the likelihood of head injury arising from an impact. In 1998, the Alliance of Automobile Manufacturers proposed the Injury Assessment Reference Value (IARV), a safe limit of the HIC value in the event of accident, to be set at 700. Head injuries would be unlikely to occur when the  $HIC_{15}$  value is below 700 [3].

Although the injury limit is not mentioned in the *Formula SAE Rules*, it is desirable to evaluate the safety of ITB's formula SAE race car structure based on an analysis of possible head injuries due to frontal collision. In the present work, frontal crash simulations were conducted to determine the effect of impact speed on the HIC value of the occupant. LS-DYNA<sup>®</sup>, an explicit finite element code for non-linear dynamic analysis, was utilized in the analysis.

## 2 Head Injury Criterion

The Head Injury Criterion (HIC) as a widely used parameter today to evaluate head injury due to accidents has a historical basis in the work of Gadd from 1961 [12], who introduced what is known as the Gadd Severity Index (GSI). Later, Versace in a study to review the GSI [13] proposed a version of the current HIC in 1971 as a measure of average acceleration that correlates with the Wayne State Tolerance Curve [14]. The HIC is defined as in Eq. (1):

$$HIC = \left\{ \left[ \frac{1}{t_2 - t_1} \int_{t_1}^{t_2} a(t) dt \right]^{2.5} (t_2 - t_1) \right\}_{max} \quad (1)$$

$$a(t) = \sqrt{a_x^2 + a_y^2 + a_z^2} \quad (2)$$

where  $a(t)$  in Eq. (2) is the head acceleration resultant and  $t_2 - t_1$  is the portion of the waveform to be measured during which HIC reaches maximum value. The US National Highway Traffic Safety Administration (NHTSA) final rule

specifies the maximum time for calculating the HIC value ( $t_2-t_1$ ) as 15 milliseconds ( $HIC_{15}$ ) [15].

The HIC has been adopted in the design of automotive head protection equipment, such as helmets. This criterion is also used by Federal Motor Vehicle Safety Standard (FMVSS) 214 as one of the criteria to assess head injuries. Payne [10] has conducted a study to find the correlation between HIC values and brain and skull fracture injury levels. The results are shown in Tables 1 and 2.

**Table 1** Proposed HIC tolerance levels correlated to brain injury [10].

Injury level	Proposed tolerance level $HIC_{15}$
0 (No concussion)	< 150
1 (No concussion)	< 150
2 (Mild concussion)	150-500
3 (Severe concussion)	500-1800
4 (Life threatening)	> 1800

**Table 2** Proposed HIC tolerance levels correlated to skull fracture [10].

Injury Level	Proposed Tolerance Level $HIC_{15}$
0 (No fracture)	< 500
1 (No fracture)	< 500
2 (Minor fracture)	500-900
3 (Major fracture)	900-1800
4 (Life threatening)	> 1800

### 3 Modeling

#### 3.1 Race Car Model

A model of ITB's FSAE race car is shown in Figure 1. To simplify the simulation process, only the main components of the car were modeled, i.e. impact attenuator (IA), anti-intrusion (AI) plate, tires, frames, engine, a-arm and cockpit. The mass distribution of the car is given in Table 3. An additional mass of 23.5 kg was given to represent the mass of small components and to round up the mass of the car to 300 kg so that frontal crash simulations with conditions as stated in the FSAE rules could be conducted.

### 3.2 Material Properties

The impact attenuator used in the race car was made of aluminum honeycomb (Plascore, Inc.) with properties and dynamic response (stress vs. volumetric strain) given in Table 4 and Figure 2, respectively. Other components, such as the frame, were made of AISI 4130, while the anti-intrusion plate and cockpit were made of aluminum 5052-H34. Their properties are given in Table 5.

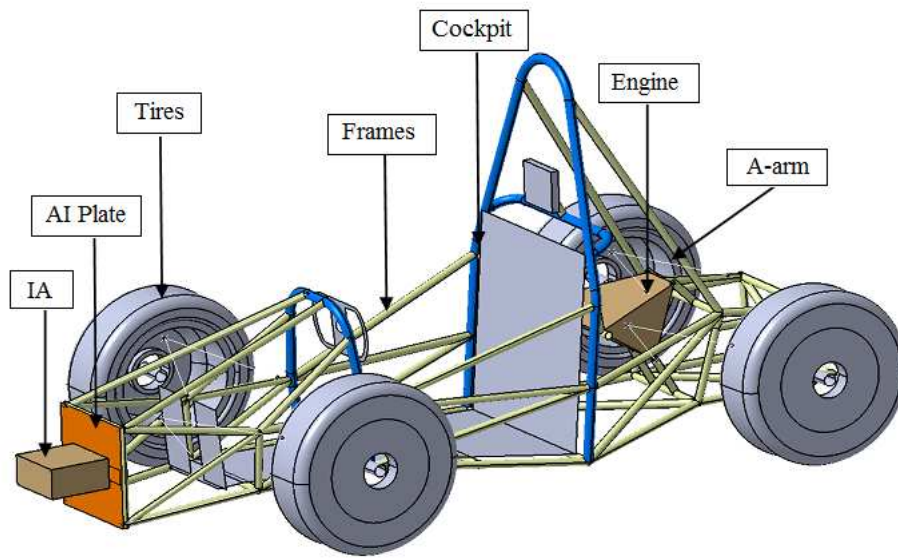


**Figure 1** ITB's FSAE race car model.

**Table 3** Mass distribution.

Component	Mass (kg)
Frames, IA, AI plate, a-arm	47
Tires	72
Engine	70
Driver	79
Cockpit	8.5
Misc (additional mass)	23.5

**Table 4** Mechanical properties of Aluminum honeycomb [16].

Properties	Value
Modulus Young (GPa)	70
Density ( $\text{kg/m}^3$ )	91
Poisson's ratio, $\nu$	0.33
Yield strength (MPa)	220
Crush strength (MPa)	2.82

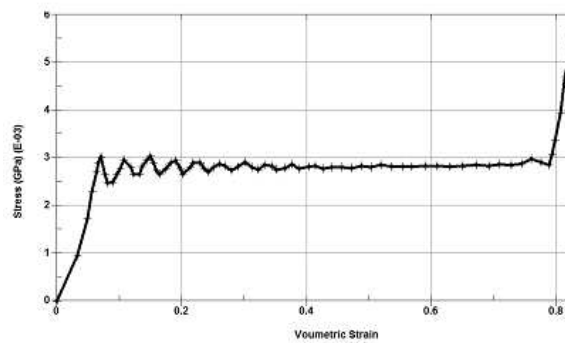


**Figure 2** Stress vs. volumetric strain curve of impact attenuator [16].

**Table 5** Mechanical properties of AISI 4130 and Aluminum 5052-H34.

<i>Properties</i>	<i>AISI 4130</i> [17]	<i>Aluminum 5052</i> [18]
Modulus Young (GPa)	205	70
Density (kg/m <sup>3</sup> )	7850	2680
Poisson's ratio, $\nu$	0.29	0.33
Yield strength (MPa)	435	214
Ultimate strength (MPa)	670	262
Fail strain	25.5%	10%

### 3.3 Finite Element Model

A finite element model of the race car is shown in Figure 3. Frames, tires, anti-intrusion plate and cockpit were all modeled by shell elements. The other components such as the impact attenuator and engine were modeled by solid elements, while the a-arms were modeled by beam elements.

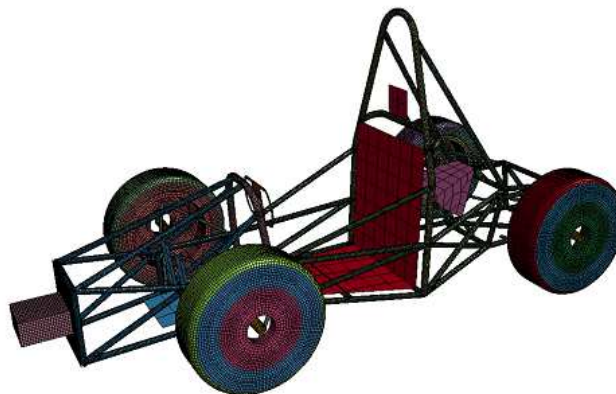


**Figure 3** Finite element model of the race car.

As for the driver, a finite element model of the *Hybrid III 50th Percentile Male Sitting* dummy was utilized. This model was jointly developed by LSTC (Livermore Software Technology Corporation) and NCAC (National Crash Analysis Center) at the George Washington University as available in [19]. The dummy is shown in Figure 4.

A finite element model of the safety belt (*Simpson*<sup>®</sup>), consisting of 2 shoulder belts, 2 lap belts, 2 anti-submarine belts and a buckle, is shown in Figure 5. The belts and the buckle were modeled by shell and solid elements respectively. The seatbelt was made of polyester with properties such as stress and strain curves as given in [20]. The contacts between belts and dummy were defined as CONTACT\_AUTOMATIC\_SURFACE\_TO\_SURFACE, with static and dynamic friction coefficients as 0.2 and 0.15, respectively.

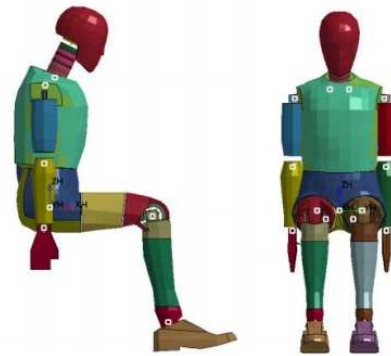


**Figure 4** Hybrid III 50th Percentile Male Sitting model [19].

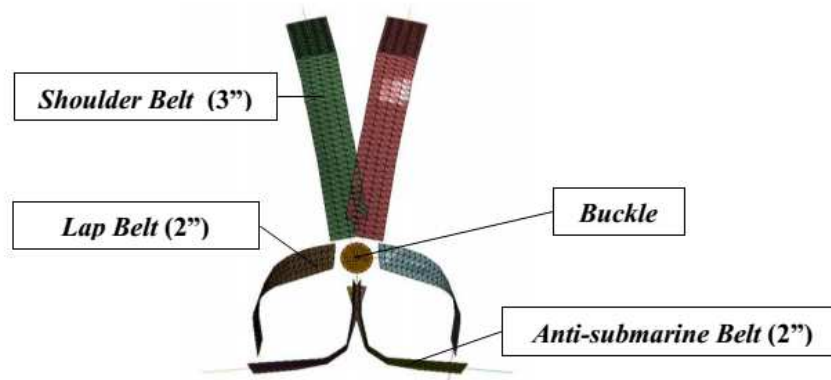


**Figure 5** Safety belt model (the number indicates the width of the belt in inches).

#### 4 Frontal Crash Simulation

In the first step, a full-frontal barrier test was simulated, as illustrated in Figure 6. In this test, the race car was run into a rigid wall with a given velocity, starting from 7 m/s until 15 m/s with 1 m/s increment. The dummy was represented by a mass element attached to the seat. Gravitational load was also applied to all elements. An accelerometer was put at the center of gravity to record the deceleration of the car. Channel frequency class (CFC) 60 was then used to filter the obtained curve.

In the second simulation, a sled test simulation, only the cockpit and dummy with seatbelt were modeled, as depicted in Figure 7. Both the cockpit and the dummy were given the initial velocity and gravitational load. Then the cockpit was decelerated using the deceleration curve obtained from the previous test. Due to this deceleration, the head was accelerated to the front while the body was constrained by the seatbelt. The head acceleration curve obtained from this test was used to calculate the  $HIC_{15}$  value.

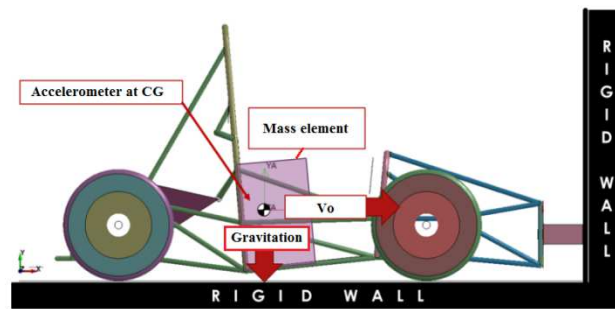


**Figure 6** Full frontal barrier test.

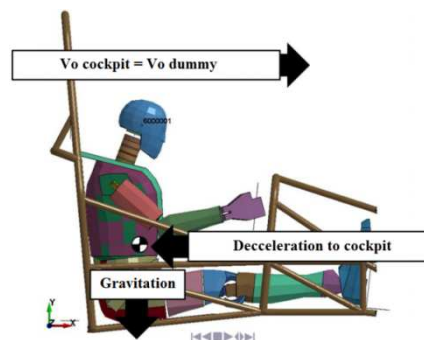


**Figure 7** Sled test.

## 5 Results and Discussion

### 5.1 Validation

To check the accuracy of the simulation results, the reaction force in the rigid wall obtained from the full frontal barrier test was evaluated. A quasi-static test of the impact attenuator was conducted. The set-up is depicted in Figure 8. As shown in the figure, an LVDT was used to measure the displacement while the reaction force (crushing force) was measured by the load cell. The results are shown in Figure 9. The solid line represents the reaction force obtained from the simulation, while the dashed line represents the quasi-static test.

From the results it can be seen that the difference in mean crushing force between the simulation and the quasi-static test was around 16%. Moisey [21] in his study about honeycomb modeling found that the difference between dynamic simulation results and the quasi-static tests was around 20% to 30%. In a few cases the differences were 10%.

As shown in Table 4, the crush strength of the impact attenuator was 2.82 MPa. Since the contact area of the impact attenuator is known ( $0.02 \text{ m}^2$ ), the mean crushing force could be easily calculated. It was found to be 56,400 N. Comparing this value with the simulation result, the difference was only 6.4%.

From the above comparisons it can be concluded that the frontal crash simulation conducted in the present study could deliver good and reasonable results.

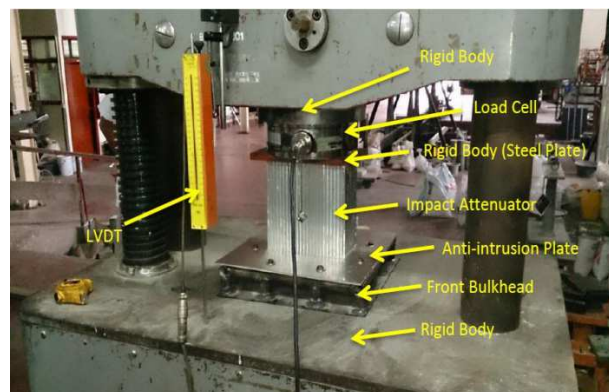


**Figure 8** Quasi static test set-up.



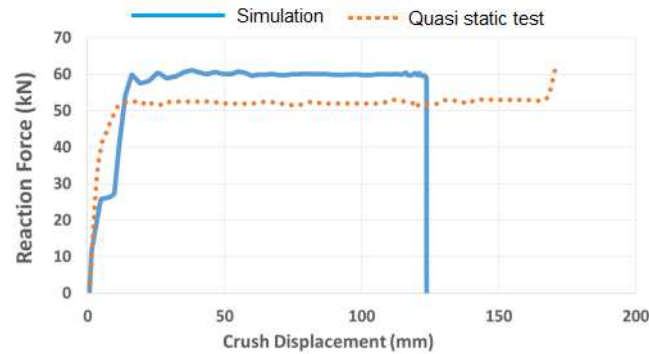


**Figure 9** Reaction forces.

## 5.2 Effect of Impact Speed

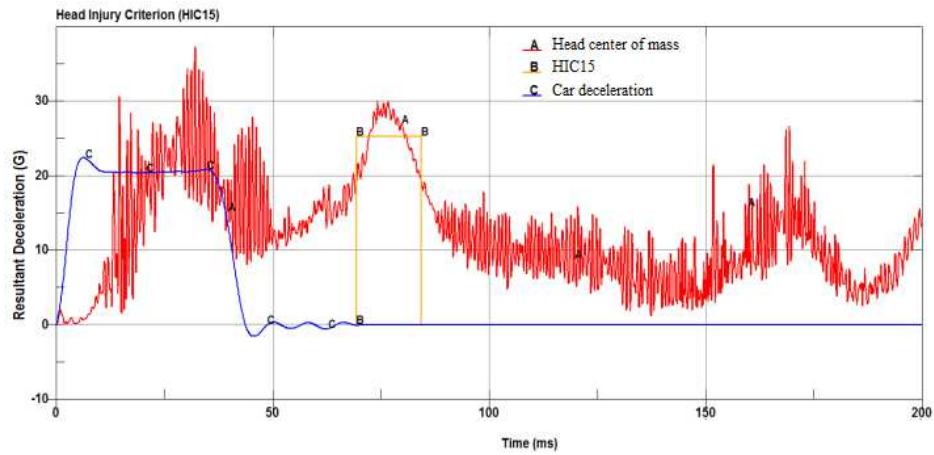
Typical head acceleration and car deceleration curves due to impact are shown in Figure 10. It can be seen that when the car is decelerated, the head begins to accelerate. The head acceleration is then briefly suspended due to the seatbelt until 50 milliseconds. However, when the body is fully restrained by the seatbelt the head begins to accelerate again. This second peak of head acceleration is generally higher than the first peak.  $HIC_{15}$  is calculated in this second peak.

Table 6 shows the average and peak decelerations of the race car as a function of impact speed. It can be seen that at 7 m/s impact speed the impact attenuator could fulfill the criteria as regulated in the 2013 Formula SAE Rules, where the average deceleration and peak deceleration of the car should be less than 20 G and 40 G respectively. This is also true for an impact speed of 8 m/s, but not for impact speeds greater than that. It is also shown that there is a sudden jump in the peak deceleration value at impact speeds of greater than 9 m/s. This occurs because the honeycomb impact attenuator has been fully compacted and there is no more room for any deformation in the honeycomb.

From the acceleration curves as shown in Figure 10, the  $HIC_{15}$  values were then calculated for all impact speeds. Figure 11 shows the calculated  $HIC_{15}$  values against impact speed.

From the figure it can be seen that at an impact speed of equal to or less than 11 m/s (39.6 km/h), the  $HIC_{15}$  values were still below the IARV (700). However, starting from 9 m/s impact speed, the  $HIC_{15}$  values steeply increased. This is due to the fact that the impact attenuator could no longer absorb the impact energy from that point on. The  $HIC_{15}$  value goes beyond the safe limit when the

impact speed is equal to or greater than 12 m/s (43 km/h). At this condition, the head may experience severe concussion.



**Figure 10** Head and car deceleration curves due to an impact speed of 7 m/s.

**Table 6** Effect of Impact Speed on Race Car Deceleration

Speed (m/s)	7	8	9	10	11	12	13	14	15
Average deceleration (G)	15.6	17.7	20.5	23.8	25.7	28.1	30.2	32.1	34.0
Peak deceleration (G)	22.4	22.6	28.8	107.5	145.0	153.0	143.4	142.5	140.1

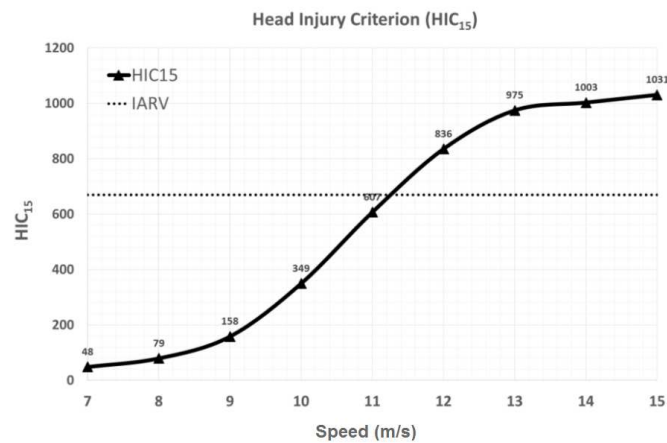


**Figure 11** HIC<sub>15</sub> vs. impact speed.

## 6 Conclusions

A study to evaluate the safety of ITB's FSAE race car and to analyze possible head injuries due to frontal collision was conducted. A reconstruction of frontal collision with an impact speed of 7 m/s to 15 m/s was made by developing a finite element model of the race car, a rigid wall, a dummy and a seatbelt. In the full frontal barrier test only the race car and rigid wall were modeled, without incorporating the dummy inside the car. The effect of impact speed on car deceleration was analyzed in this step. In the sled test simulation, only the cockpit, the dummy and the seatbelts were modeled, where the deceleration curves obtained from the full frontal barrier test were used as input. The effect of car deceleration on head injury was then analyzed.

From the results it was found that the impact attenuator of ITB's FSAE race car fulfilled the safety criteria as regulated in the 2013 Formula SAE Rules. Analysis of the effect of impact speed on the possibility of occupant head injury shows that  $HIC_{15}$  values at an impact speed of 7 m/s (25 km/h) to 11 m/s (40 km/h) are still within the safe zone (below the IARV). However, the  $HIC_{15}$  value will exceed the safe limit when the speed of impact is the same as or greater than 12 m/s (43 km/h).

## References

- [1] Society of Automotive Engineers, *2013 Formula SAE® Rules*, FSAE, 2013.
- [2] *General Statistic: Passenger Vehicle Occupant*, IIHS, <http://www.iihs.org/iihs/topics/t/general-statistics/fatalityfacts/passenger-vehicles#Crash-types>, 10 August 2015.
- [3] Mertz, H.J., *Injury Risk Assessments Based on Dummy Responses*, Accidental Injury: Biomechanics and Prevention 2nd Edition, Nahum, A.M. & Melvin, J.W. (ed.), New York: Springer, pp. 89-102, 2002.
- [4] Tatsuya, F., Hiroshi, E., Yusuke, M. & Shinobu, S., *Effect of Seat Belt Positions on Passenger Injury during Low Speed Front-end Impact*, Kanazawa University, SAE International, 2009.
- [5] Schmitt, K-U., Niederer, P.F., Muser, M.H. & Walz, F., *Trauma Biomechanics Accidental Injury in Traffic and Sports: 2nd Edition*, Springer, 2007.
- [6] Pasternak & Zirgibel, S.C., *Car Accident Injuries*, [http://www.frankpasternak.com/car\\_accident\\_injuries.htm](http://www.frankpasternak.com/car_accident_injuries.htm), (10 August 2015).
- [7] Gennarelli, T.A. & Wodzin, E., (ed.), *The Abbreviated Injury Scale 2005*, Barrington, IL: Association for the Advancement of Automotive Medicine; 2005.

- [8] Patel, A. & Goswami, T., *Comparison of Intracranial Pressure by Lateral and Frontal Impacts - Validation of Computational Model*, Injury and Skeletal Biomechanics, Goswami, T. (ed.), Intech, pp. 95-114, 2012.
- [9] Cory, C.Z., Jones, M.D., James, D.S., Leadbeatter, S., Nokes, L.D.M., *The Potential and Limitations of Utilising Head Impact Injury Models to Assess the Likelihood of Significant Head Injury in Infants After a Fall*, Forensic Science International, **123**(2-3), pp. 89-106, 2001.
- [10] Payne, A.R., *Head Injury Criteria Tolerance Levels*, <http://www.eurailsafe.net/subsites/operas/HTML/Section3/Page3.3.1.4.htm>, 10 August 2015.
- [11] Du Bois, P., Chou, C.C., Fileta, B.B., Khalil, T.B., King, A.I., Mahmood, H.F., Mertz, H.J. & Wismans, J., *Vehicle Crashworthiness and Occupant Protection*, Michigan, AISI, 2000.
- [12] Gadd, C.W., *Criteria for Injury Potential*, Impact Acceleration Stress Symposium, National Research Council publication, 977, National Academy of Sciences, Washington DC, pp 141-144, 1961.
- [13] Versace, J., *A Review of the Severity Index*, Proceeding 15th Stapp Car Crash Conference, SAE paper 710881, pp. 771-796, 1971.
- [14] Lissner, H.R., Lebow, M. & Evans, F.G., *Experimental Studies on the Relation Between Acceleration and Intracranial Pressure Changes in Man*, Surgery, Gynecology, and Obstetrics, **111**, pp. 329-338, 1960.
- [15] Eppinger, R., Sun, E., Kuppa, S. & Saul, R., *Development of Improved Injury Criteria for the Assessment of Advanced Automotive Restraint Systems – II*, National Highway Traffic Safety Administration, U.S. Department of Transportation, Washington, DC., 2000.
- [16] Plascore, *Certificate of Conformance: Aluminum Honeycomb PAMG-XR1-5.2-3/16-N-5052*, Plascore, 2013.
- [17] ASM Aerospace Specification Metals Inc., *AISI 4130 Steel*, <http://asm.matweb.com/search/SpecificMaterial.asp?bassnum=m4130r>, (10 August 2015).
- [18] ASM Aerospace Specification Metals Inc., *Aluminum 5052-H34*, <http://asm.matweb.com/search/SpecificMaterial.asp?bassnum=MA5052H34>, (10 August 2015).
- [19] Livermore Software Technology Corporation, *LSTC Dummy and Barrier Models for LS-DYNA*, [http://www.lstc.com/download/dummy\\_and\\_barrier\\_models](http://www.lstc.com/download/dummy_and_barrier_models), 10 August 2015.
- [20] Doug D., *Simpson Performance Products: Safety First*, <https://simpsonraceproducts.com/pdf/SafetyFirst9-03.pdf>, 10 August 2015.
- [21] Shkolnikov, M.B., *Honeycomb Modeling for Side Impact Moving Deformable Barrier (MDB)*, 7th International LS-DYNA Users Conference, Dearborn, Michigan, United States, 2002.